Bone Hydration Affects Toughness: A Quasi-Brittle Fracture Mechanics Perspective

Glynn Gallaway[1], Joseph M. Wallace[2], Matthew R. Allen[3], John Howarter[4], Laura J. Pyrak-Nolte[5], Thomas Siegmund[1]
[1]School of Mechanical Engineering, Purdue University, W. Lafayette, IN, [2]Department of Biomedical Engineering, Indiana University Purdue University Indianapolis, Indianapolis, IN, [3]Department of Anatomy, Cell Biology, and Physiology, Indiana University School of Medicine, Indianapolis, IN, [4]School of Materials Science and Engineering, Purdue University, W. Lafayette, IN, [4]Depatment of Physics and Astronomy, Purdue University, W. Lafayette, IN
ggallawa@purdue.edu

Disclosures: No Disclosures.

INTRODUCTION: Bone toughness has often been evaluated using either linear elastic fracture mechanics (LEFM) concepts or a J-integral approach. However, bone exhibits several behaviors that negate the assumptions for both approaches. Most prominently, bone has been shown to have a fracture process zone (FPZ) of significant size [1]. An FPZ is the volume in front of the crack tip where some damage has occurred, but the material is not fully fractured. To most holistically assess toughness, the FPZ size must be accounted for relative to the specimen dimension. Quasi-brittle fracture mechanics (QBFM) incorporates these measures, which has been applied to bovine bone [2] but not in humans. Raloxifene (RAL), a selective estrogen receptor modulator, which has been found to change bone hydration and improve toughness in human, canine, and murine specimens [3,4]. This work evaluates changes in bone toughness in response to RAL treatment in both the linear elastic and quasi-brittle framework.

METHODS: Human cortical femur tissue was obtained through the Indiana School of Medicine Anatomical Donation Program from a 75-year-old male. Bones were into nominally 4 x 4 x 24 mm^3 beams sectioned using a low-speed saw with a diamond blade. A 200 µm notch was cut into the endosteal side of the beam. Here, 8 beams are considered under 3 treatment conditions: 3 beams treated in a 2 µM RAL solution, 2 beams treated in a vehicle control solution (VEH) [2], and 3 beams in their native (NAT) state only exposed to PBS. An in-situ loading and 3D imaging approach was used for fracture experiments. Notched beams were loaded under four-point bending (lower span = 16 mm) at a rate of 0.1 mm/min while in a bath of PBS using a Deben 5 kN CT load cell situated in a Zeiss XRADIA 3D X-Ray Microscope. During loading, 2D X-Ray images were obtained to track crack mouth opening displacement ($CMOD$). Loading was stopped at peak load and the displacement was held constant while a 3D X-Ray image was obtained using 2401 projections with 5s exposure at a voxel size of 4.2 µm. Images from the 3D scan were reconstructed in the XRADIA workflow and analyzed in Simpleware ScanIP to determine the size of the FPZ, FPZ. The LEFM toughness, G_{LEFM}, is calculated with respect to the initial crack length, a_0. For QBFM, toughness, G_{QBFM}, is computed from an effective crack length, a_{eff}. Effective crack length is $a_0 + FPZ/2$, or is alternatively calculated from $CMOD$ and force in 2D images [5]. The extension of the crack from a_0 defines the fracture process zone length. In the following equations, P_{max} is the maximum load, E' is the plane strain Young's modulus of the bone (19.8 GPa), B and D are the width and depth of the beam, respectively, and $g(a_i/D)$ is a dimensionless shape function for notched four-point bending.

$$G_{LEFM} = \frac{P_{max}^2}{E'B^2D} g\left(\frac{a_0}{D}\right) \qquad G_{QBFM} = \frac{P_{max}^2}{E'B^2D} g\left(\frac{a_{eff}}{D}\right)$$

RESULTS: Image based FPZ lengths and effective FPZ lengths from $CMOD$ methods for each treatment group are shown in Figure 1. FPZ length was highest with RAL; image-based methods measure a maximum geometric FPZ and CMOD methods measure an effective FPZ. In Figure 2, 3D images show the shape and size of the FPZ within one representative sample. A tortuous crack is observed that interacts with the osteon structure. Results of the elastic and quasi-brittle toughness of each sample are shown in Figure 3. The median G_{LEFM} for RAL, VEH, and NAT samples were 0.87, 1.02, and 0.68 N/mm, respectively. The median G_{QBFM}^{CMOD} for RAL, VEH, and NAT samples were 3.07, 2.53, and 1.87 N/mm, respectively. The median G_{QBFM}^{img} for RAL, VEH, and NAT samples were 1.84, 1.54, and 1.19 N/mm, respectively. The significance of the difference for: G_{LEFM} between RAL and NAT is p = 0.32; G_{QBFM}^{img} between RAL and NAT is p = 0.13; G_{QBFM}^{CMOD} for RAL and NAT is p = 0.07.

DISCUSSION: The current results are limited to a small cohort; additional experiments are on-going. The FPZ size is significant relative to the size of the beam and the osteon microstructure ($FPZ \approx 3 \times$ 0n. Dm) which indicates dependence of toughness on the FPZ. The quasi-brittle approach indicates a higher toughness as compared to LEFM. Fracture process zone size is larger in RAL-treated samples in both methods of determining an effective crack length. RAL-treated specimens are also shown to have a higher linear elastic toughness, a higher quasi-brittle toughness, and a larger relative increase in toughness from LEFM to QBFM when compared to the native samples using both image and $CMOD$ based effective crack lengths. These results indicate that RAL appears as to enhance the quasi-brittle toughening mechanisms in human cortical bone.

SIGNIFICANCE/CLINICAL RELEVANCE: Direct measurement of the large fracture process zone in bone indicates a significant size effect which will be important to consider in experimental studies of bone toughness. Application of quasi-brittle methods to human bone can provide a new perspective on toughness, that is a function of maximum pad and damage accumulated, and lead to better treatments of bone disease.

REFERENCES: [1] Koester, KJ, et al., *Nat. Mater.*, 2008;7:672-677 [2] Kim, KT, et al., *Int. J. Fract.*, 2013;181:67-81 [3] Gallant, MA, et al., *Bone*, 2014;61:191-200 [4] Surowiec, RK, et al., *Bone*, 2023;173: 116805 [5] Yangyang, Y, et al., *Eng. Fract. Mech.*, 2019; 211:371-381

ACKNOWLEDGEMENTS: Supported by NSF (CMMI) grant 1952993. G.G. supported by NSF-GRF DGE-1842166 and Purdue Doctoral Fellowship.

IMAGES AND TABLES:

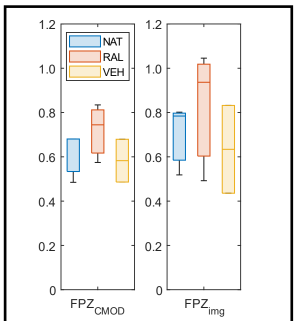

Figure 1. FPZ measures (mm)

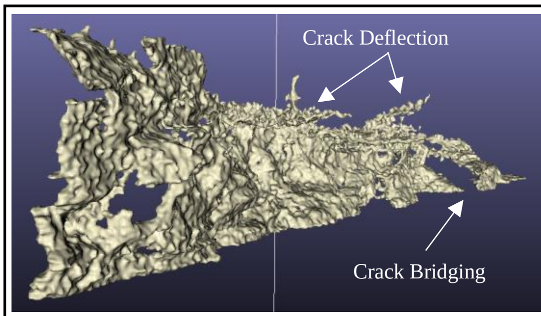

Figure 2. 3D segmentation of crack front in one sample

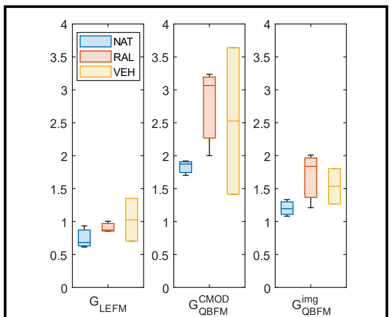

Figure 3. Toughness measures (N/mm)